INTERNATIONAL TRANSACTIONS IN OPERATIONAL RESEARCH

Intl. Trans. in Op. Res. XX (20XX) 1–16
DOI: xx.xxxx/itor.xxxxx

An automated treatment planning strategy for highly noncoplanar radiotherapy arc trajectories

P. Carrasqueira[a,*], H. Rocha[a,b], J. M. Dias[a,b], T. Ventura[a,c], B. C. Ferreira[a,d] and M. C. Lopes[a,c]

[a]*INESCC, Rua Silvio Lima, 3030-290 Coimbra, Portugal*
[b]*CeBER and FEUC, Av. Dias da Silva 165, 3004–512 Coimbra, Portugal*
[c]*IPOC-FG, EPE, Av. Bissaya Barreto 98, 3000–075 Coimbra, Portugal*
[d]*ESS.PP, Rua Valente Perfeito 322, 4400–330 Vila Nova de Gaia, Portugal*
E-mail: pedro.carrasqueira@deec.uc.pt [P. Carrasqueira]; hrocha@mat.uc.pt [H. Rocha]; joana@fe.uc.pt [J. M. Dias]; tiagoventura@ipocoimbra.min-saude.pt [T. Ventura]; bcf@ess.ipp.pt [B. C. Ferreira]; mclopes@ipocoimbra.min-saude.pt [M. C. Lopes]

Received DD MMMM YYYY; received in revised form DD MMMM YYYY; accepted DD MMMM YYYY

Abstract

Radiation therapy is a technology-driven cancer treatment modality that has experienced significant advances over the last decades, thanks to multidisciplinary contributions that include engineering and computing. Recent technological developments allow the use of noncoplanar volumetric arc therapy (VMAT), one of the most recent photon treatment techniques, in clinical practice. In this work, an automated noncoplanar arc trajectory optimization framework designed in two modular phases is presented. First, a noncoplanar beam angle optimization algorithm is used to obtain a set of noncoplanar irradiation directions. Then, anchored in these directions, an optimization strategy is proposed to compute an optimal arc trajectory. Treatment plans obtained considering the optimized noncoplanar arc trajectories, for a pool of twelve difficult head-and-neck tumor cases, present a remarkable quality improvement when compared with treatment plans obtained considering coplanar equispaced beam directions, still commonly used in clinical practice. Furthermore, significant quality improvements were obtained for some of the cases when compared to coplanar VMAT treatment plans. Automated procedures like the one proposed in this paper will simplify the current treatment workflow, making better use of human resources and allowing for unbiased comparisons between different treatment techniques. As running the proposed automated framework will not waste any human resources, it can be assessed as being a valuable tool in clinical practice even if it only benefits specific patients.

Keywords: Radiation therapy; Noncoplanar arc therapy; Optimization; Automation

*Author to whom all correspondence should be addressed (e-mail: pedro.carrasqueira@deec.uc.pt).

1. Introduction

Cancer continues to be an increasing health problem with an expected increase of 63.1% of cancer cases by 2040, compared with 2018 (WHO). In high-income countries, photon radiation therapy (RT) is used in more than half of all cancer cases (Atun et al., 2015). The goal of RT is to eliminate all cancerous cells by irradiating the tumor volume(s) (PTVs) with a prescribed radiation dose while trying to spare the surrounding organs at risk (OARs) as much as possible. In external RT, radiation is generated by a linear accelerator mounted on a gantry able to rotate around the patient that lays immobilized in a treatment couch that can also rotate around a vertical axis that intersects the gantry rotation horizontal axis at a point called the isocenter. The rotation of the couch and the gantry allows the irradiation of the tumor from almost any direction. The possibility of selecting appropriate noncoplanar irradiation directions – noncoplanar beam angle optimization (BAO) problem – can enhance treatment plan quality, particularly for complex tumor sites as head-and-neck cancer cases (Bangert et al., 2013).

RT has seen considerable changes in the last decades, offering an increased range of treatment techniques to cancer patients. The most advanced RT systems use a multileaf collimator (MLC) to modulate the radiation beam into a discrete set of small beamlets with different intensities. The beamlets intensities can be optimized – fluence map optimization (FMO) problem – leading to nonuniform radiation fields that can be delivered while the gantry is halted at given beam irradiation directions, static intensity-modulated radiation therapy (IMRT), or can be delivered while the gantry rotates around the patient with the treatment beam always on, rotational/arc IMRT. Volumetric modulated arc therapy (VMAT) is one of the most efficient IMRT arc techniques, particularly with respect to dose delivery time (Otto, 2008). Typically, VMAT uses coplanar beam trajectories, performed for a fixed couch angle (usually 0°).

Recent technological advances give additional degrees of freedom to treatment planning. Moving simultaneously the gantry and the couch, provided collisions are avoided, has become a reality for the most recent line of linear accelerators. Highly noncoplanar arc trajectories can now be obtained as couch rotation is allowed while the gantry rotates around the patient. Recently, the use of highly noncoplanar trajectories was proposed to combine the benefits of VMAT, such as short treatment times (Otto, 2008), with the benefits of noncoplanar IMRT treatment plans, such as improved organ sparing (Bangert et al., 2013).

Designing a complete end to end noncoplanar VMAT treatment plan, requires different optimization problems to be addressed, related to beam angle selection, fluence map optimization and trajectory optimization, in order to increase treatment plan quality. To obtain a deliverable treatment plan it is also needed to adapt the treatment plan to specific constraints of the machine. In Yang et al. (2011) a new method is presented to deal with dynamic movement of gantry and couch, as the dose is being delivered to the patient. A geometric based score is proposed to measure the OARs overlapping the tumor indicating promising trajectories. Hierarchical clustering is then used to construct multiple subarcs with continuous gantry and couch rotation. MacDonald and Thomas (2015) embedded beams-eye-view dose metrics, i.e. metrics related to the percent of PTV and OARs seen from each beam direction, in their arc trajectory optimization. Smyth et al. (2016) also considered a geometric based heuristic to select noncoplanar beams, relying on a cost function that evaluates the OARs superposition with the PTV, for each beam. Considering the score determined for each beam, the shortest path Dijkstra algorithm is used to design the final noncoplanar trajectory. This technique makes some improvements on the approach presented in Smyth et al. (2013), namely assigning different weights to each OAR according to its rela-

tive importance. Papp et al. (2015) presented an approach to obtain noncoplanar VMAT treatment plans that starts by performing beam angle selection resorting to two FMO heuristics. The beam trajectory is obtained by optimizing distances considered as the sum of the time needed to change from one beam to the next one, for all the trajectory, resorting to a shortest path algorithm. In Wild et al. (2015) the noncoplanar VMAT trajectories were constructed using genetic algorithms to solve the shortest path problem, based on the anchor points given by the beams of noncoplanar IMRT plans. Langhans et al. (2018) designed a strategy to perform noncoplanar BAO and then uses a geometrical based metric to find an optimized arc trajectory.

As far as the authors know, fully FMO based strategies to determine arc therapy trajectories have not been explored so far. In this paper, a completely automated approach to obtain a noncoplanar VMAT treatment plan is developed. Initially, a noncoplanar beam angle optimized solution is determined lying on a strategy early developed (Rocha et al., 2016, 2019a). Anchored on the noncoplanar beam directions calculated, an automated fluence based optimization framework is proposed for obtaining an optimal noncoplanar arc trajectory plan. An experimental direct aperture optimization implementation provided by matRad (Wieser et al., 2017) is used for fluence optimization that guide both BAO and trajectory optimization, aiming at minimizing the possible discrepancies to fully deliverable VMAT plans. The approach herein presented is assessed in a group of 12 head-and-neck cancer patients already treated at the Portuguese Institute of Oncology of Coimbra (IPOC). This paper is organized as follows. In section 2, the head-and-neck cancer cases used to assess the proposed approach are presented. The trajectory optimization framework is described in section 3. In section 4, the computational results are presented. The last section is devoted to the conclusions.

2. Head-and-neck cancer cases

Twelve head-and-neck complex tumor cases already treated at IPOC were simultaneously considered to test the proposed automated approach. Two different dose prescription levels were considered for each patient. A higher radiation dose of 70.0 Gy was prescribed to the tumor (PTV_{70}) while a lower radiation dose of 59.4 Gy was prescribed to the lymph nodes ($PTV_{59.4}$).

Treatment planning of head-and-neck cancer cases is difficult due to the large number of OARs surrounding both the tumor and the lymph nodes. Parotid glands, oral cavity, spinal cord and brainstem compose the list of OARs considered. The larger salivary glands, left and right parotids, and the oral cavity, that contains the remaining salivary glands, are parallel organs, i.e. organs whose functionality is not impaired if only a small part is damaged. Thus, mean-dose constraints are considered for parallel organs. Spinal cord and brainstem are serial organs, i.e. organs that may see their functionality impaired even if only a small part is damaged. Thus, maximum-dose constraints are considered for serial organs. A structure containing the remaining normal tissues, Body, is also considered to prevent dose accumulation elsewhere. Table 1 depicts the prescribed doses for the PTVs and the tolerance doses for the OARs considered.

Table 1
Prescribed doses for the PTVs and tolerance doses for the OARs considered.

Structure	Prescribed	Tolerance Dose	
	dose	Mean	Max
$\mathbf{PTV_{70}}$	70.0 Gy	–	–
$\mathbf{PTV_{59.4}}$	59.4 Gy	–	–
Left parotid	–	26 Gy	–
Right parotid	–	26 Gy	–
Oral cavity	–	45 Gy	–
Spinal cord	–	–	45 Gy
Brainstem	–	–	54 Gy
Body	–	–	80 Gy

3. Noncoplanar arc trajectory optimization framework

The proposed arc trajectory optimization framework is an automated modular process which evolves in two steps. In the first step, a set of optimal noncoplanar beam irradiation directions is obtained, resorting to a previously developed BAO algorithm (Rocha et al., 2016, 2019a). In the second step, anchored in the previously computed beams directions, additional beam directions are iteratively calculated in order to define the noncoplanar arc trajectory. The optimization procedures of both steps are guided by the optimal value of the fluence optimization problem. Direct aperture optimization is used in this work for fluence optimization rather than the conventional beamlet-based fluence optimization commonly used, including in our preliminary work done manually for a nasopharyngeal tumor case to assess the effectiveness of a fluence based arc trajectory calculation (Rocha et al., 2019b). Next, the fluence optimization approach used in this work is presented followed by the description of the two steps that compose the framework.

3.1. Fluence map optimization – direct aperture optimization

In arc therapy, the gantry rotates around the patient with the beam always on while the gantry speed, the dose rate, and the aperture shaped by the MLC are modulated. Figure 1 illustrates a MLC with different aperture shapes and the corresponding radiation maps whose superimposition originates a nonlinear fluence map. Conventional fluence optimization calculates the optimal intensities of each beamlet that produce the nonlinear intensity map. In order to be deliverable, another optimization step is required to calculate the sequence of apertures (sequencing) that approximately reproduce the optimal nonlinear fluence maps. Direct aperture optimization (DAO) calculates aperture shapes instead of beamlet intensities producing a deliverable plan. The use of DAO during treatment planning can thus decrease possible discrepancies to fully deliverable VMAT plans.

The head-and-neck clinical cases considered in this work were assessed in matRad (Wieser et al., 2017). matRad is an open source multi-modality radiation treatment planning system, written in Matlab, developed at the German Cancer Research Center. Core functionalities comprised in matRad include

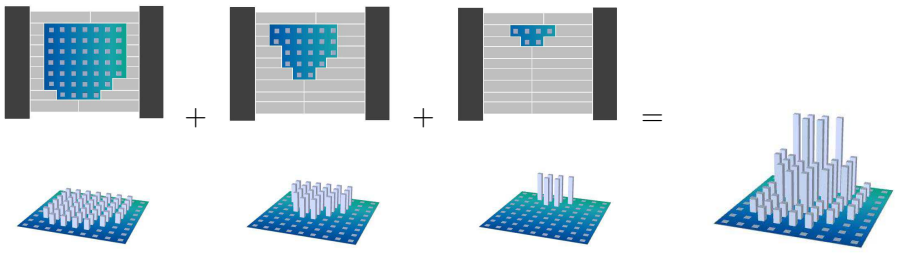

Figure 1. Illustration of a MLC with different apertures and corresponding radiation maps whose superimposition originate a nonlinear fluence map.

importing DICOM data, dose calculation and optimization as well as a graphical user interface for visualization. It comprehends twofold usage, writing customized Matlab scripts or using matRad GUI, which provides a straightforward process to obtain a treatment plan through a completely automated procedure. Fluence optimization in matRad may be customized selecting, from a set of options available, objectives, constraints or weights assigned to each structure. Thus, matRad provides sufficient freedom to design a custom optimization procedure in an automated fashion. Furthermore, matRad provides an experimental DAO implementation which was the main motivation to use this software in this work. matRad uses a gradient-based DAO algorithm (Cassioli and Unkelbach, 2013) that depends on a good starting solution. Therefore, a conventional fluence optimization including sequencing (Xia and Verhey, 1998) is first performed and the resulting segments are then refined based on gradient information (Wieser et al., 2017).

In this work, a convex voxel-based nonlinear model (Aleman et al., 2008; Yang and Xing, 2004) is used for fluence optimization by selecting the appropriate options in matRad. In this model, the objective function accounts for the overall penalization considering the weighted sum of square deviation of the dose deposited in each voxel relatively to the dose prescribed for that voxel. This evaluation is performed for each structure s of the S structures considered. The mathematical formulation results in a quadratic programming problem. For each structure s, the objective function is formulated as

$$f_s(w) = \underline{\lambda}_s(T_s - \sum_{j=1}^{N_b} D_{ij}w_j)_+^2 + \overline{\lambda}_s(\sum_{j=1}^{N_b} D_{ij}w_j - T_s)_+^2 \tag{1}$$

where D_{ij} is the unitary dose delivered to voxel i by beamlet j, w_j is the weight (intensity) of beamlet j, T_s is the prescribed/tolerance dose of structure s, N_b is the number of beamlets, $\underline{\lambda}_s$ and $\overline{\lambda}_s$ are the lower and upper penalties for the structure s and $(\cdot)_+ = \max\{0, \cdot\}$. The under dosage has not been penalized for OARs, which means setting $\underline{\lambda}_s$ null for those structures. Each structure s was assigned an importance rank k_s. The FMO model is obtained by the weighted sum of the all objective functions defined for the structures, which is formulated as

$$\begin{aligned} \min_w \quad & f = \sum_{s=1}^{S} k_s f_s(w) \\ s.t. \quad & w_j \geq 0, j = 1, \ldots, N_b. \end{aligned} \tag{2}$$

In matRad, the fluence optimization problem is solved resorting to the interior point optimizer solver IPOPT (Wächter, 2006) which is a reliable free software package developed by the COIN-OR initiative fitted to solve large scale nonlinear constrained optimization problems. IPOPT is made available by a MEX file, which resorts on the objective functions and constraints defined within the matRad environment.

3.2. Noncoplanar beam angle selection

In clinical practice, equispaced coplanar irradiation directions are still commonly used, i.e. beam irradiation directions evenly distributed on the plane of rotation of the linear accelerators gantry. The main reason for the clinical use of equispaced beam angle ensembles is inherent to the challenge of solving the BAO problem, a non-convex problem with many local minima on a large search space (Craft, 2007). The vast majority of the approaches proposed to address the BAO problem consider a discrete subset of all continuous beam angle directions solving the resulting combinatorial optimization problem (Aleman et al., 2008; Bertsimas et al., 2013; Cabrera et al., 2018; Craft, 2007; Dias et al., 2014, 2015; Freitas et al.; Lim and Cao, 2012), either relying on geometric measures or in dosimetric values. However, the optimal solution of the combinatorial BAO problem cannot be calculated in a polynomial run time – NP hard problem (Bangert et al., 2012). We proposed an alternative BAO formulation. Instead of considering a discrete subset of beam directions, all continuous beam angle directions are considered leading to a continuous global optimization problem (Rocha et al., 2016, 2019a). The continuous formulation and resolution of the noncoplanar BAO problem is briefly described next.

Considering the goal of obtaining a beam ensemble with n beams and assuming that θ stands for the gantry angle and ϕ for the couch angle, the noncoplanar BAO problem can be simply formulated as

$$\begin{aligned} \min \quad & f\Big((\theta_1,\phi_1),(\theta_2,\phi_2),\ldots,(\theta_n,\phi_n)\Big) \\ s.t. \quad & (\theta_1,\phi_1),(\theta_2,\phi_2),\ldots,(\theta_n,\phi_n) \in A, \end{aligned}$$

where $A = \{(\theta,\phi) : \theta \in [0,360],\ \phi \in [-90,90]\}$. The objective function, f, for which the best beam ensemble is attained at the function's minimum has been considered by us as the optimal value of the FMO problem. Here, the optimal value of the DAO problem described in the previous section will guide the noncoplanar BAO search. In a noncoplanar setting some beam directions cannot be considered as collision between gantry and couch or patient may occur. To accomplish this situation the objective function f is formulated as

$$f\Big((\theta_1,\phi_1),\ldots,(\theta_n,\phi_n)\Big) = \begin{cases} \text{optimal DAO value} & \text{if no collisions occur} \\ +\infty & \text{otherwise.} \end{cases}$$

In terms of BAO (or DAO) optimization, the order of each beam in the beam ensemble is irrelevant as all the beam ensembles with the same beam directions, even disposed in a different order, correspond to the exact same solution. Thus, the BAO search space can be largely reduced by keeping the beam directions sorted, reducing substantially the computational effort of the BAO search. To implement this

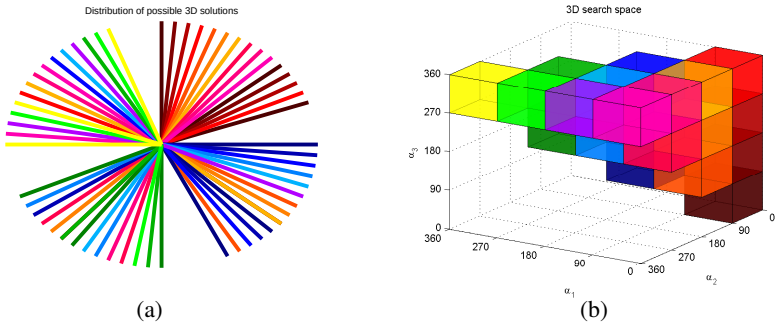

(a) (b)

Figure 2. All possible sorted combinations of three-beam ensembles divided by quadrant – 2(a) and the corresponding cubes in the reduced 3-D BAO search space – 2(b).

strategy, the overall search space is split into hypercubes of one quadrant length. For illustration purposes, in Fig. 2(a) are represented all the possible combinations of three-beam ensembles by quadrant. In Fig. 2(b) the corresponding cubes (reduced search space) are depicted. This partition of the reduced search space proved to be useful for a straightforward multistart sampling strategy that considers an initial beam ensemble for each of the hypercubes. Depending on the dimension of the optimization problem (number of beams), each of the hypercubes is still a large search region, with possibly many local minima, that should be explored resorting to derivative-free optimization methods to avoid local entrapment (Rocha et al., 2013c,a,b). Furthermore, each of the hypercubes can be considered as a region of attraction to prevent overlapping of the local hypercube searches. Algorithms 1 and 2 depict the derivative-free algorithm to locally explore each hypercube and the multistart algorithm, respectively. For further details see Rocha et al. (2016, 2019a).

3.3. Noncoplanar arc trajectory optimization

The optimization approach proposed for calculating noncoplanar arc trajectories is anchored in the beam directions obtained by the BAO algorithm, adding iteratively novel anchor directions considering optimal DAO values. When 20 anchor beams are obtained, which is the typical number of anchor beams considered in the literature to define the trajectory path (Papp et al., 2015; Wild et al., 2015), this iterative procedure ends. The automated noncoplanar arc trajectory optimization is now described considering one of the head-and-neck cancer cases to illustrate the optimization strategy proposed.

Figure 3 displays in red, both in 2D (3(a)) and in 3D (3(b)), the 7-beam ensemble, solution of the noncoplanar BAO problem for one of the head-and-neck cancer cases tested. Note that each beam direction is represented by an ordered pair where the first coordinate refers to the gantry angle and the second to the couch angle. For the iterative optimization strategy proposed, an equispaced beam grid separated by 10° for both the gantry and the couch is considered and the corresponding beams are displayed in black for 0° couch angles, which typically corresponds to coplanar plans, or blue for different couch angle values. Infeasible beams due to possible collisions of couch and gantry for a head-and-neck cancer case

Algorithm 1 Parallel derivative-free algorithm

Initialization:

- Set $k \leftarrow 0$;
- Set $\mathbf{x}^0$ as the current best beam ensemble of a given hypercube;
- Set α_0 as the current step-size parameter for the corresponding hypercube;
- Set α_{min} to the same value defined in Algorithm 2;

Iteration:

1. Compute in parallel $f(\mathbf{x})$, the optimal DAO value, for all beam ensembles $\mathbf{x}$: $\mathbf{x} \in \mathcal{N}(\mathbf{x}^k) = \{\mathbf{x}^k \pm \alpha_k v_j, v_j \in [I \ -I]\}$, where $I = [e_1 \dots e_n]$ is the identity matrix.
2. If $\min_{\mathcal{N}(\mathbf{x}^k)} f(\mathbf{x}) < f(\mathbf{x}^k)$ then
   $\mathbf{x}^{k+1} \leftarrow \text{argmin}_{\mathcal{N}(\mathbf{x}^k)} \text{f}(\mathbf{x})$;
   $\alpha_{k+1} \leftarrow \alpha_k$;
   Else
   $\mathbf{x}^{k+1} \leftarrow \mathbf{x}^k$;
   $\alpha_{k+1} \leftarrow \frac{\alpha_k}{2}$;
3. If $\alpha_{k+1} \geq \alpha_{min}$ return to step 1 for a new iteration and set $k \leftarrow k + 1$.

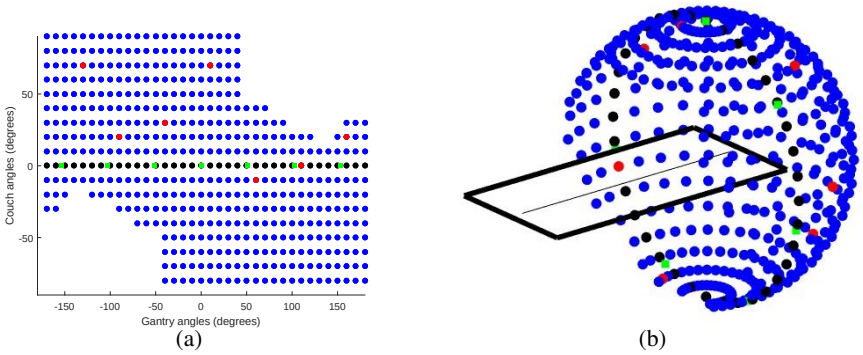

(a) (b)

Figure 3. Equispaced beam grid represented in 2D – 3(a) and the corresponding 3D representation – 3(b). Red beams correspond to the BAO solution, green beams to the 7-beam coplanar equispaced solution, black beams correspond to 0° couch angles (coplanar plans) while blue beams correspond to different couch values.

were excluded as represented in Figure 3.

Similarly to the BAO approach, the arc trajectory optimization approach is based on dosimetric considerations, and will be guided by the optimal values of the DAO problem. Apart from geometric features, one of the criteria commonly used for calculating noncoplanar arc trajectories is delivery time. Aiming at enhancing one of the main VMAT features, short delivery times, the gantry/couch movements are constrained according to the follow conditions:

Algorithm 2 Parallel multistart algorithm

Initialization:

- Set $k \leftarrow 0$;
- Choose the initial beam ensembles $\mathbf{x}_i^0$, one for each of the N hycubes of the reduced search space;
- Compute $f(\mathbf{x}_i^0), i = 1, \ldots, N$, the optimal DAO value for the initial beam ensembles, in parallel;
- Set the best beam ensembles as $\mathbf{x}_i^* \leftarrow \mathbf{x}_i^0, i = 1, \ldots, N$ and the best optimal DAO values in each hypercube as $f_i^* \leftarrow f(\mathbf{x}_i^0), i = 1, \ldots, N$;
- Set all the hypercubes as regions of attraction having active local searches, $\mathbf{Active}_i \leftarrow 1, i = 1, \ldots, N$;
- Choose initial step-size, $\alpha_i^0 > 0, i = 1, \ldots, N$;
- Set α_{min} to the same value defined in Algorithm 1;

Iteration:

1. Use Algorithm 1 to locally explore the hypercubes with active local search;
2. For hypercubes i with active local search do
   If $f(\mathbf{x}_i^{k+1}) < f(\mathbf{x}_i^*)$ then
      If $\mathbf{x}_i^{k+1}$ is in cube i then
         $\mathbf{x}_i^* \leftarrow \mathbf{x}_i^{k+1}$;
         $f_i^* \leftarrow f(\mathbf{x}_i^{k+1})$;
      Else (local search "jump" to a different hypercube)
         $\mathbf{Active}_i \leftarrow 0$;
         Determine hypercube $j \neq i$ where $\mathbf{x}_i^{k+1}$ is;
         If $f(\mathbf{x}_i^{k+1}) < f(\mathbf{x}_j^*)$ then
            $\mathbf{x}_j^* \leftarrow \mathbf{x}_i^{k+1}$;
            $f_j^* \leftarrow f(\mathbf{x}_i^{k+1})$;
            $\mathbf{Active}_j \leftarrow 1$;
   Else
      $\alpha_i^{k+1} \leftarrow \frac{\alpha_i^k}{2}$;
      If $\alpha_i^{k+1} < \alpha_{min}$ then
         $\mathbf{Active}_i \leftarrow 0$;
3. If there exists active hypercubes return to step 1 and set $k \leftarrow k + 1$.

- The initial gantry/couch position is the leftmost anchor beam in Fig. 3(a), corresponding to the beam of the noncoplanar BAO solution with lowest value of gantry angle;
- The anchor beam to visit next has the lowest gantry angle value among the ones that have not been visited yet;
- The final gantry/couch position is the rightmost anchor beam in Fig. 3(a), corresponding to the beam of the noncoplanar BAO solution with highest value of gantry angle;
- The gantry must always move towards the next anchor beam while the couch can move towards the next anchor beam or be halted.

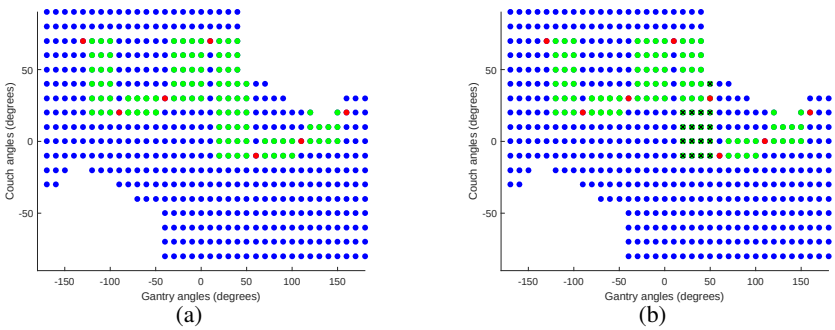

Figure 4. The 7-beam noncoplanar BAO solution is displayed in red and the feasible points to consider when calculating a new anchor beam are displayed in green – 4(a). Novel anchor beam belonging to the largest set of green candidate beams is added and green candidate beams that became infeasible are removed – 4(b).

By imposing these movement constraints, the arc trajectory is defined from the leftmost anchor beam to the rightmost anchor beam of Figure 3(a) as fast as possible, i.e., with the gantry always moving towards the next anchor beam and the couch also moving (when necessary) towards the next anchor beam. These movement constraints present yet another advantage. The number of feasible beams to consider when computing the next anchor beam is reduced. The candidate beams to consider when calculating a new anchor beam are colored green in Figure 4(a). The most populated set is selected for searching the new anchor beam to add to the current arc trajectory. The rationale behind this idea is threefold: to reduce the computational time, to add anchor beams where more degrees of freedom exist and to reduce as much as possible the overall number of green points. After selecting the set of beams to test, each candidate beam is temporarily inserted in the trajectory and the optimal DAO value for the corresponding beam ensemble is calculated. The beam ensemble reporting the best performance is selected to become the updated arc trajectory. Then, the sets of eligible beams are updated and the largest one is selected for searching the new beam to add to the current arc trajectory. Figure 4(b) illustrate one iteration of this arc trajectory optimization approach. This iterative procedure ends when the number of anchor beams is 20. The process of obtaining the optimized arc trajectory has been completely automated in order to get the required solution without additional human intervention. The pseudocode of the arc trajectory optimization algorithm is presented in Algorithm 3.

4. Computational results

An eight-core Dell Precision T5600 with Intel Xeon processador was used and the computational tests were hosted by matRad workstation. Objective functions displayed in Eq. 1 were implemented in matRad by selecting the appropriate options. Higher importance ranks, k_s, were assigned to PTVs in Eq. 2, followed by the OARs. The lowest importance rank was assigned to remaining normal tissues (Body). The BAO algorithm considered $\alpha_0 = 2^5 = 32$ as initial step size and define as stopping criteria a step size inferior to one. By choosing a power of two for initial step size and one for minimum step

Algorithm 3 Noncoplanar arc trajectory algorithm

Initialization:

- Set the initial anchor beams to the BAO solution found;
- Calculate the candidate beams to be tested as novel anchor beams;

Iteration:

While candidate beams exist **and** number of anchor beams is less than 20 **do**

1. Identify the largest set of candidate green beams between two anchor beams;
2. Compute the optimal DAO value considering the set of beams composed of the anchor beams and each candidate beam identified in the previous step;
3. Add a novel anchor beam corresponding to the candidate beam that leads to the best optimal DAO value in the previous step;
4. Remove the green candidate beams that became infeasible.

size, all beam angle directions considered will be integer since the step size is divided by two in case of an unsuccessful local search.

The quality of the treatment plans obtained by the automated framework, called *ncVMAT*, was compared with coplanar VMAT plans, called *cVMAT*, with static noncoplanar IMRT plans considering the beam ensembles obtained by the BAO procedure, called *ncIMRT*, and with equispaced coplanar static IMRT plan, called *cIMRT*, still commonly used in clinical practice. Figure 5 displays the highly noncoplanar trajectory obtained by our arc trajectory optimization framework.

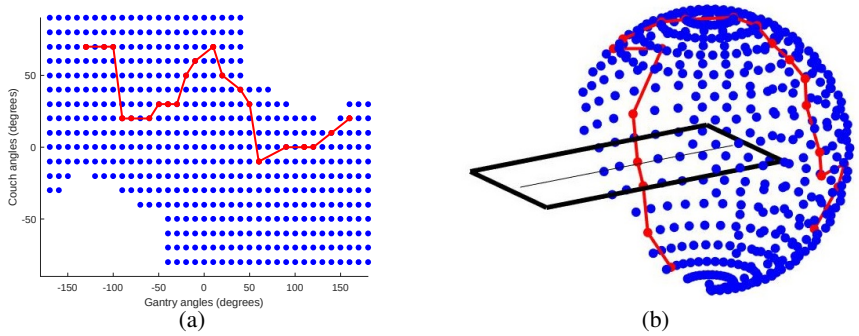

Figure 5. Trajectory obtained by the noncoplanar arc trajectory optimization framework in 2D – 5(a) and in 3D – 5(b).

The comparison of the different approaches was performed in terms of the optimal objective function value as well as resorting to different dosimetric measures typically used to assess the quality of treatment plans. The optimal FMO values obtained for each of the approaches tested are presented in Table 2. *ncVMAT* treatment plans clearly outperform the other treatment plans in terms of optimal FMO value, improving on average 31.1% the value obtained by the benchmark treatment plan, *cIMRT*, while the

Table 2
Results in terms of optimal FMO value for the 12 cases.

	cIMRT	*cVMAT*		*ncIMRT*		*ncVMAT*	
Case	FMO value	FMO value	% decrease	FMO value	% decrease	FMO value	% decrease
1	141.1	134.7	4.5	136.5	3.3	129.7	8.0
2	39.0	27.3	29.8	33.1	15.2	25.8	33.8
3	238.1	213.6	10.3	218.4	8.3	208.7	12.4
4	179.9	161.3	10.3	168.1	6.6	157.7	12.4
5	68.0	40.6	40.3	47.7	29.8	39.1	42.5
6	109.3	101.5	7.1	104.4	4.4	98.5	9.9
7	45.6	32.9	27.9	35.4	22.2	29.0	36.4
8	41.2	27.3	33.8	25.3	38.5	21.7	47.4
9	8.0	5.5	31.3	6.9	12.9	5.5	31.1
10	37.0	22.0	40.6	25.5	31.0	21.2	42.6
11	32.1	19.0	40.6	20.6	35.8	14.7	54.1
12	20.1	14.5	27.9	15.4	23.3	11.5	42.9

improvements of *ncIMRT* and *cVMAT* were 19.3% and 25.4%, respectively.

Despite the excellent results obtained in terms of optimal objective function values, as the objective functions used in fluence optimization models do not have a clinical meaning and it is not possible to fully correlate its value with physical dose objectives or clinical response, other metrics are typically used to assess the quality of treatment plans: D95 for the PTVs and maximum and mean doses for the serial and parallel OARs, respectively. D95 measures the dose delivered to at least 95% of the PTVs. D95 should be at least 95% of the prescribed dose. Comparison of PTV coverage metrics (D95) obtained by *cIMRT*, *cVMAT*, *ncIMRT* and *ncVMAT* treatment plans is displayed in Figure 6 while comparison of organ sparing metrics is displayed in Figure 7. It is possible to observe that in terms of coverage metrics both for tumor (PTV_{70}) and lymph nodes ($PTV_{59.4}$), *ncVMAT* clearly outperforms the remaining approaches. It is worth to highlight that *ncVMAT* it is the only plan that can meet the tumor ($PTV70$) prescription for the fourth patient. In terms of organ sparing, results obtained by the different plans fulfill most of the times the tolerance doses with no clear advantage of one approach for all structures. For instance, for spinal cord *ncVMAT* obtained the best sparing with an average 1.8 Gy decrease with respect to the benchmark treatment plan, *cIMRT*, while for brainstem *cVMAT* obtained the best sparing with an average 1.8 Gy decrease with respect to *cIMRT*.

5. Conclusions

In this paper a novel automated framework was proposed to determine optimized noncoplanar arc trajectories to deliver radiation therapy to cancer patients. Two very challenging problems just by themselves, the noncoplanar beam angle selection and the noncoplanar arc trajectory optimization, were combined in the proposed optimization framework. Both optimization procedures were guided by the optimal

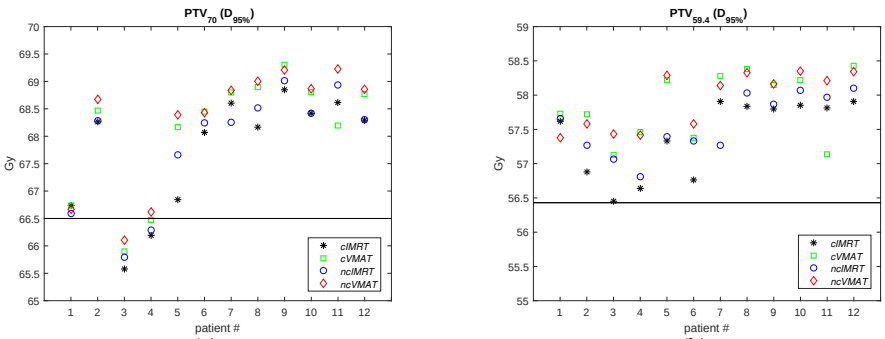

Figure 6. Comparison of PTV coverage metrics (D95) obtained by *cIMRT*, *cVMAT*, *ncIMRT* and *ncVMAT* treatment plans. The horizontal lines displayed represent D_{95}.

values of an experimental DAO implementation provided by matRad, aiming at minimizing discrepancies to fully deliverable VMAT plans.

The quality of the treatment plans obtained by the automated framework, *ncVMAT*, was assessed using a pool of 12 difficult head-and-neck cancer cases already treated at IPOC. Comparison with coplanar VMAT plans, *cVMAT*, noncoplanar IMRT plans, *ncIMRT*, and benchmark equispaced coplanar IMRT plans, *cIMRT*, was clearly favorable in terms of optimal objective function values obtained. In terms of dosimetric measures typically inspected to assess the quality of a treatment plan, *ncVMAT* also outperforms clearly the remaining approaches. In terms of organ sparing, the results are not so clear with advantage of different approaches for different structures and for different patients. The choice of higher importance ranks, k_s, for PTVs might explain the better performance of the optimized angular approaches in terms of these structures. Nevertheless, for some patients *ncVMAT* obtained the best results not only in terms of target coverage but also in terms of organ sparing for most of the OARs. For instance, for patient four, *ncVMAT* obtained not only better target coverage results than the remaining approaches that fail to achieve 95% of the prescribed dose for D95 of PTV_{70}, but also better sparing of spinal cord, brainstem, oral cavity and right parotid, fulfilling the tolerance doses for left parotid and Body. Note that only plans with noncoplanar optimized directions fulfilled the mean dose limit imposed to right parotid. As the tumor volume (PTV_{70}) is overlapping the right parotid, the selection of appropriate irradiation directions proved to be important for this particular case.

In Europe, currently, less than 75% of the patients that should be treated with radiotherapy actually are (Lievens et al., 2019). One of the reasons is the time required for treatment planning of complex tumor cases that is still nowadays a trial and error process that can take long hours to days for a medical physicist to complete. Automated procedures like the one proposed in this paper will not only simplify the current treatment workflow, making better use of the existing human resources, but it will also allow for unbiased comparisons between different treatment techniques. As running the proposed automated framework will not waste any human resources, even if it only benefits specific patients, it can be assessed as being a valuable tool in clinical practice.

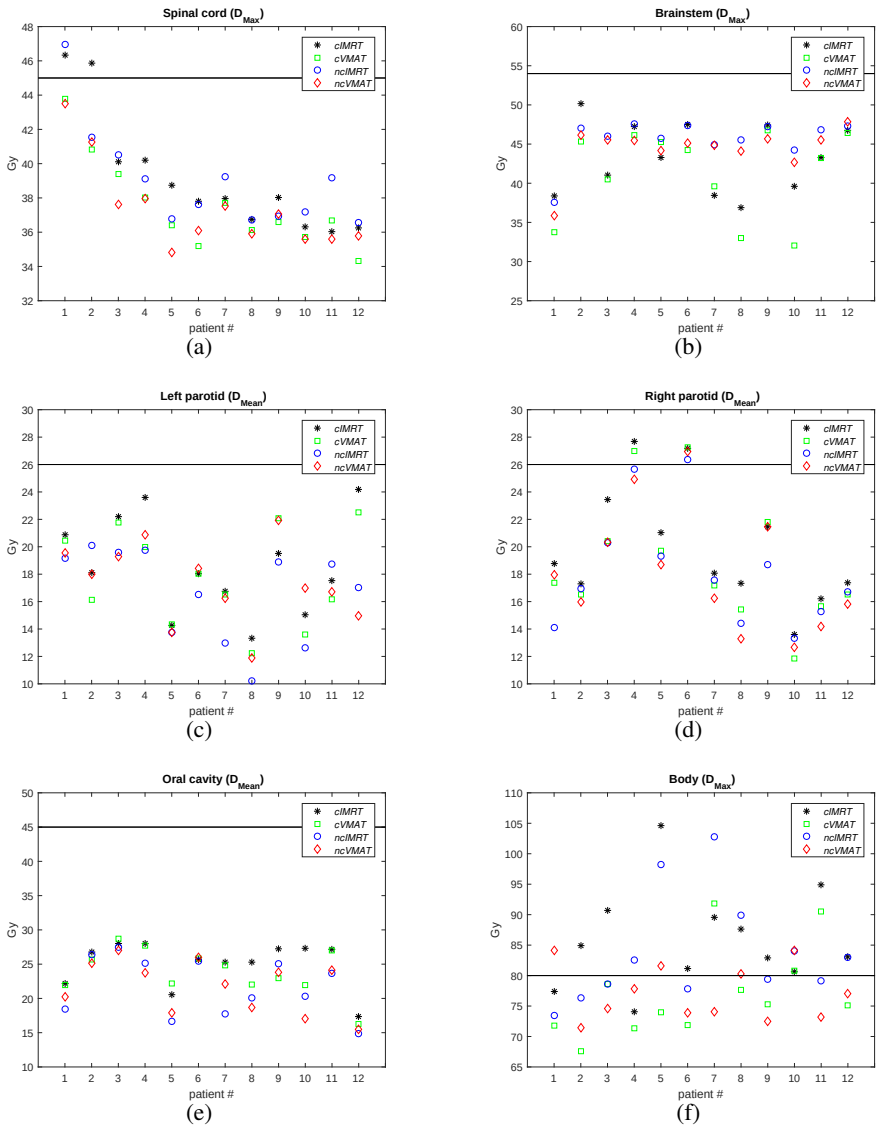

Figure 7. Comparison of organ sparing metrics obtained by *cIMRT*, *cVMAT*, *ncIMRT* and *ncVMAT* treatment plans. The horizontal lines displayed represent the tolerance (mean or maximum) dose for each structure.

Acknowledgments.

This work has been supported by project grant POCI-01-0145-FEDER-028030 and by the Fundação para a Ciência e a Tecnologia (FCT) under project grants UIDB/05037/2020 and UIDB/00308/2020.

References

Aleman, D., Kumar, A., Ahuja, R., Romeijn, H., Dempsey, J., 2008. Neighborhood search approaches to beam orientation optimization in intensity modulated radiation therapy treatment planning. *J. Global Optim.* 42, 587–607.

Atun, R., Jaffray, D., Barton, M., Bray, F., Baumann, M., Vikram, B., Hanna, T., Knaul, F., Lievens, Y., Lui, T., 2015. Expanding global access to radiotherapy. *Lancet Oncol.* 16, 1153–1186.

Bangert, M., Ziegenhein, P., Oelfke, U., 2012. Characterizing the combinatorial beam angle selection problem. *Phys. Med. Biol.* 57, 6707–6723.

Bangert, M., Ziegenhein, P., Oelfke, U., 2013. Comparison of beam angle selection strategies for intracranial imrt. *Med. Phys.* 40, 011716.

Bertsimas, D., Cacchiani, V., Craft, D., Nohadani, O., 2013. A hybrid approach to beam angle optimization in intensity-modulated radiation therapy. *Comput. Oper. Res.* 40, 2187–2197.

Cabrera, G., Ehrgott, M., Andrew J. Mason, A.J., Raith, A., 2018. A matheuristic approach to solve the multiobjective beam angle optimization problem in intensity-modulated radiation therapy. *Intl. Trans. Op. Res.* 25, 243–268.

Cassioli, A., Unkelbach, J., 2013. Aperture shape optimization for imrt treatment planning. *Phys. Med. Biol.* 58, 301–318.

Craft, D., 2007. Local beam angle optimization with linear programming and gradient search. *Phys. Med. Biol.* 52, 127–135.

Dias, J., Rocha, H., Ferreira, B., Lopes, M., 2014. A genetic algorithm with neural network fitness function evaluation for imrt beam angle optimization. *Cent. Eur. J. Oper. Res.* 22, 431–455.

Dias, J., Rocha, H., Ferreira, B., Lopes, M., 2015. Simulated annealing applied to imrt beam angle optimization: A computational study. *Phys. Med.* 31, 747–756.

Freitas, J., Florentino, H., Benedito, A., Cantane, D., . Optimization model applied to radiotherapy planning problem with dose intensity and beam choice. *Appl. Math. Comput.* (in press).

Langhans, M., Unkelbach, J., Bortfeld, T., Craft, D., 2018. Optimizing highly noncoplanar vmat trajectories: the novo method. *Phys. Med. Biol.* 63, 025023.

Lievens, Y., Ricardi, U., Poortmans, P., Verellen, D., Gasparotto, C., Verfaillie, C., Cortese, A., 2019. Radiation oncology. optimal health for all, together. estro vision, 2030. *Radiother. Oncol.* 136, 86–97.

Lim, G., Cao, W., 2012. A two-phase method for selecting imrt treatment beam angles: Branch-and-prune and local neighborhood search. *Eur. J. Oper. Res.* 217, 609–618.

MacDonald, R.L., Thomas, C.G., 2015. Dynamic trajectory-based couch motion for improvement of radiation therapy trajectories in cranial srt. *Med. Phys.* 42, 2317–2325.

Otto, K., 2008. Volumetric modulated arc therapy: Imrt in a single gantry arc. *Med. Phys.* 35, 310–317.

Papp, D., Bortfeld, T., Unkelbach, J., 2015. A modular approach to intensity-modulated arc therapy optimization with noncoplanar trajectories. *Phys. Med. Biol.* 60, 5179–5198.

Rocha, H., J., D., Ferreira, B., Lopes, M., 2013a. Beam angle optimization for intensity-modulated radiation therapy using a guided pattern search method. *Phys. Med. Biol.* 58, 2939–53.

Rocha, H., J., D., Ferreira, B., Lopes, M., 2013b. Pattern search methods framework for beam angle optimization in radiotherapy design. *Appl. Math. Comput.* 219, 10853–65.

Rocha, H., J., D., Ferreira, B., Lopes, M., 2013c. Selection of intensity modulated radiation therapy treatment beam directions using radial basis functions within a pattern search methods framework. *J. Glob. Optim.* 57, 1065–89.

Rocha, H., J., D., Ventura, T., Ferreira, B., Lopes, M., 2016. A derivative-free multistart framework for an automated noncoplanar beam angle optimization in imrt. *Med. Phys.* 43, 5514–5526.

Rocha, H., J., D., Ventura, T., Ferreira, B., Lopes, M., 2019a. Beam angle optimization in imrt: are we really optimizing what matters? *Intl. Trans. Op. Res.* 26, 908–928.

Rocha, H., J., D., Ventura, T., Ferreira, B., Lopes, M., 2019b. An optimization approach for noncoplanar intensity-modulated arc therapy trajectories. In *19th International Conference on Computational Science and Its Applications*, LNCS, Springer, pp. 199–214.

Smyth, G., Bamber, J., Evans, P., Bedford, J., 2013. Trajectory optimisation for dynamic couch rotation during volumetric modulated arc radiotherapy. *Phys. Med. Biol.* 58, 8163–8177.

Smyth, G., Evans, P., Bamber, J., Mandeville, H., Welsh, L., Saran, F., Bedford, J., 2016. Non-coplanar trajectories to improve organ at risk sparing in volumetric modulated arc therapy for primary brain tumors. *Radiother. Oncol.* 121, 124–131.

Wächter, .B.L. A., 2006. On the implementation of an interior-point

filter line-search algorithm for large-scale nonlinear programming. *Math. Program.* 106, 25–57.

WHO, 2020. Cancer tomorrow. http://gco.iarc.fr/tomorrow/home. Accessed: 2020-02-10.

Wieser, H.P., Cisternas, E., Wahl, N., Ulrich, S., Stadler, A., Mescher, H., Muller, L., T., K., Gabrys, H., Burigo, L., Mairani, A., Ecker, S., Ackermann, B., Ellerbrock, M., Parodi, K., Jakel, O., Bangert, M., 2017. Development of the open-source dose calculation and optimization toolkit matrad. *Med. Phys.* 44, 2556–2568.

Wild, E., Bangert, M., Nill, S., Oelfke, U., 2015. Noncoplanar vmat for nasopharyngeal tumors: Plan quality versus treatment time. *Med. Phys.* 42, 2157–2168.

Xia, P., Verhey, L., 1998. Multileaf collimator leaf sequencing algorithm for intensity modulated beams with multiple static segments. *Med. Phys.* 25, 1424–1434.

Yang, Y., Xing, L., 2004. Inverse treatment planning with adaptively evolving voxel-dependent penalty scheme. *Med. Phys.* 31, 2839–2844.

Yang, Y., Zhang, P., Happersett, L., Xiong, J., Yang, J., Chan, M., Beal, K., Mageras, G., Hunt, M., 2011. Choreographing couch and collimator in volumetric modulated arc therapy. *Int. J. Radiat. Oncol. Biol. Phys.* 80, 1238–1247.